Near-Wall Turbulent Flows
R.M.C. So, C.G. Speziale and B.E. Launder (Editors)

The application of low Reynolds number k-ε models to mass and momentum transport in the inner and outer wall regions

D.J. Bergstrom[a], J.W. Gu[a], S. Nesic[b] and J. Postlethwaite[b]

[a] Department of Mechanical Engineering, University of Saskatchewan, Saskatoon, Saskatchewan, S7N 0W0, Canada

[b] Department of Chemical Engineering, University of Saskatchewan, Saskatoon, Saskatchewan, S7N 0W0, Canada

Abstract

The present paper examines the use of low Reynolds number k-ε models to predict mass and momentum transport in two different near-wall flows. A turbulent Schmidt number is used to calculate the wall mass transfer rate in fully developed channel flow. Both linear and non-linear k-ε models are used to calculate the velocity field in a plane wall jet. In each case, the low Reynolds number model represents an improvement over a wall function approach; however, important deficiencies remain.

1. INTRODUCTION

Practical engineering computations of heat and fluid flow require accurate near-wall turbulence models. Within a Reynolds average formulation, the complex flow structure in the near-wall region is represented by a smooth change in transport properties. The turbulent transport, characteristically greater than molecular diffusion, is considered to diminish as the wall is approached, so that in the immediate vicinity of the wall only viscous effects remain. However, the wall is also known to modify the transport properties in fully turbulent flow at finite distances from the wall. These two effects are often described, respectively, as 1) low Reynolds number and 2) wall-damping phenomenon. Even for as simple a flow as a flat plate boundary layer, the underlying turbulence structure in the near-wall region is remarkably complex [1], so that developing a turbulence model

which captures not only the properties but also *mimics* the structural mechanisms of the near-wall region is not a trivial task.

The past decade has seen the application of low Reynolds number (LRN) models to a wide range of engineering flows. Perhaps the most popular of these models has been the low Reynolds formulation of the k-ε model, e.g. [2,3]. Most of these models were originally developed and 'calibrated' using simple boundary layer or channel flows. The effect of the wall on the overall transport level was primarily implemented by damping the turbulent contribution as the wall was approached. As such, LRN k-ε models focus on the first effect described above, and are less able to reproduce the second.

The LRN k-ε models suffer from the limitations of the high Reynolds number 'parent' model for complex shear flows. As eddy viscosity models, it is difficult to incorporate buoyancy or curvature effects in a generally applicable manner. One limitation in near-wall flows is the approximate isotropy of the normal Reynolds stress components. The wall region itself is strongly anisotropic. One attempt to remedy this limitation, still within the context of a two-equation model, is the so called non-linear k-ε model. In this model, higher order products (in terms of the mean strain $U_{i,j}$) are introduced into the eddy viscosity relation to reproduce the anisotropy of the normal stresses. One such non-linear k-ε model, which has also been implemented in a low Reynolds number formulation, is that of Myong and Kasagi [4].

A more appropriate method for modelling complex turbulent flows is use of a second moment closure. Solving transport equations for the Reynolds stress components generally results in more accurate modelling of the turbulence structure, including the anisotropy of the near-wall region. However, this approach requires substantially more computational effort. Furthermore, although several low Reynolds number formulations have been proposed, see the review of So et al [5], they have not yet been widely tested except for simpler boundary layer type flows.

The present paper considers two different near-wall flows. Firstly, mass transfer within a fully developed channel flow for a high Schmidt number fluid is used to assess the performance of a LRN model within the viscous sublayer. The value predicted for the mass transfer rate at the wall using a constant turbulent Schmidt number is found to be within 25 percent of the empirical value. The second aspect of near-wall flows to be considered is the wall damping within the outer region of a turbulent wall jet. Use of either a linear or a non-linear LRN k-ε model is shown to be incapable of reproducing the reduction in the turbulent shear stress in the outer region. In contrast, a Reynolds stress closure is known to be capable of reproducing this effect. The two cases

considered above are examples of relatively simple flow configurations which challenge the near-wall performance of low Reynolds number k-ε closures.

2. MATHEMATICAL MODEL

The mathematical model adopted consists of the Reynolds-average form of the conservation equations for mass, momentum and a scalar property. For two-dimensional incompressible flow, the transport equations become

$$U_{i,i} = 0 \tag{1}$$

$$\rho\, U_j U_{i,j} = -p_{,i} + \rho g_i + (\mu\, U_{i,j})_{,j} - \rho\, \langle u_i u_j \rangle_{,j} \tag{2}$$

$$U_j \Theta_{,j} = (\Gamma \Theta_{,j})_{,j} - \langle u_j \theta \rangle_{,j} \tag{3}$$

where U_i is the mean velocity and Θ is a scalar property in this case the species concentration. The focus of the present study is the modelling of the Reynolds stress $\langle u_i u_j \rangle$ and turbulent scalar flux $\langle u_i \theta \rangle$.

The low Reynolds number k-ε model uses an eddy viscosity relation for the Reynolds stress, i.e.

$$\langle u_i u_j \rangle = \frac{2}{3} \delta_{ij}\, k - \nu_t\, (U_{i,j} + U_{j,i}) \tag{4}$$

where the eddy viscosity is given by the relation

$$\nu_t = c_\mu\, f_\mu\, \frac{k^2}{\varepsilon} \tag{5}$$

and k is the turbulence kinetic energy and ε is its dissipation rate. The function f_μ is a damping function which reduces the value of ν_t as the wall is approached. Transport equations are solved for both k and ε; the equations are as follows:

$$U_j k_{,j} = [(\frac{\nu_t}{\sigma_k} + \nu)\, k_{,j}]_{,j} - \langle u_i u_j \rangle\, U_{i,j} - \varepsilon \tag{6}$$

$$U_j \varepsilon_{,j} = [(\frac{\nu_t}{\sigma_\varepsilon} + \nu)\, \varepsilon_{,j}]_{,j} - c_{\varepsilon 1} f_1\, \frac{\varepsilon}{k}\, \langle u_i u_j \rangle\, U_{i,j} - c_{\varepsilon 2} f_2\, \frac{\varepsilon^2}{k} \tag{7}$$

Again, damping functions, f_1 and f_2, are introduced into the source terms of the ε equation so that the level of ε (and hence k) is modified in the near-wall region. Specific functions for f_μ, f_1 and f_2, together with the values of the model constants, are given in references [2,3].

Equation (4) can be regarded as a linear eddy viscosity model. Non-linear formulations have recently been proposed to include anisotropic effects. In the non-linear model of Myong and Kasagi [4], the expression for the Reynolds stress becomes

$$\langle u_i u_j \rangle = \frac{2}{3} k \delta_{ij} - \nu_t (U_{i,j} + U_{j,i}) + \frac{k}{\varepsilon} \nu_t \sum_{\beta=1}^{3} c_\beta (S_{\beta ij} - \frac{1}{3} S_{\beta kk} \delta_{ij})$$

$$+ \frac{2}{3} \nu \frac{k}{\varepsilon} W_{ij}(n,m) \left(\frac{\partial \sqrt{k}}{\partial x_n}\right)^2 \qquad (8a)$$

where

$$S_{1ij} = U_{i,k} U_{j,k} \qquad (8b)$$

$$S_{2ij} = \frac{1}{2} (U_{k,i} U_{j,k} + U_{k,j} U_{i,k}) \qquad (8c)$$

$$S_{3ij} = U_{k,i} U_{k,j} \qquad (8d)$$

and $W_{ij}(n,m)$ is a function defined in terms of the coordinate directions, n, normal to the wall and, m, in the streamwise direction, i.e.

$$W_{ij}(n,m) = -\delta_{ij} - \delta_{in}\delta_{jn} + 4\,\delta_{im}\delta_{jm} \qquad (8e)$$

with no summation over n or m. It is evident from equation (8) that the non-linear relation introduces a much more complex dependence of $\langle u_i u_j \rangle$ on the mean strain field.

Thus far we have considered modelling of the Reynolds stress term in the momentum equation, in the context of a LRN k-ε model. The scalar flux, $\langle u_i \theta \rangle$, is modelled in an analogous manner using an eddy diffusivity relation

$$\langle u_i \theta \rangle = - \Gamma_t \Theta_{,i} \qquad (9)$$

where the eddy diffusivity, Γ_t, is related to the eddy viscosity using a turbulent Schmidt number σ_t, i.e. $\Gamma_t = \nu_t / \sigma_t$. In many flows, the turbulent Schmidt number is assumed to be constant, even though one

would more reasonably expect it to be a function of the flow field. For the near-wall region, Kays and Crawford [6] propose a variable turbulent Prandtl/Schmidt number which is a function of the local turbulent Peclet number, $Pe_t = (\nu_t/\nu)Sc$. Using this relation, the value of σ_t at the wall is typically almost twice the value far from the wall.

3. WALL MASS TRANSFER RATE

The first near-wall transport problem to be considered is that of mass transfer within a fully developed channel flow. In many industrial systems involving aqueous solutions, the corrosion encountered at the duct wall is controlled by mass transfer. That is to say, the rate of chemical reaction at the wall is limited by the rate at which a species is transported to the wall, which in term depends on the level of molecular and turbulent diffusion. For a high Schmidt number fluid, the mass transfer boundary layer is much thinner than the hydrodynamic boundary layer. Thus, even *residual* levels of mechanical turbulence within the nominally viscous region close to the wall can result in turbulent species diffusion which overwhelms any molecular transport. As such, the mass transfer rate predicted by a numerical solution which utilizes a low Reynolds number model is especially sensitive to the reduction in the eddy viscosity deep within the near-wall region. When a turbulent Schmidt number, Γ_t, is used to model the turbulent scalar flux, any variation in Γ_t near the wall also becomes important.

Fully developed channel flow is a convenient test case in two regards. Firstly, the mathematical problem can be solved numerically without significant errors being introduced by the computation itself. Secondly, Berger and Hau [7] have developed an empirical correlation for the Stanton number for mass transfer in fully developed pipe flow, $St_d = k_d/U$, which can be used to estimate the mass transfer coefficient k_d in a channel flow with bulk velocity U.

The velocity and concentration fields were numerically solved for a turbulent channel flow using a one-dimensional finite volume code. In this case, convection could be neglected entirely and the diffusive fluxes were evaluated using a central difference approximation. The LRN model of Nagano and Tagawa [2] was used to close the mean transport equations. The physical solution domain consisted of one-half of a channel of width h = 0.4 m, with bulk velocity U = 0.406 m/s. A symmetry boundary condition was implemented at the centerline. At the wall, the velocity and turbulence kinetic energy, k, were set equal to zero, while the dissipation rate ε balanced the viscous diffusion of k. For

the aqueous solution considered, the Schmidt number was Sc = 1460. The species concentration at the centerline was $\Theta_c = 0.001$; at the wall the concentration was set equal to zero. This implied that the corrosion reaction consumed any species transported to the wall. The numerical grid consisted of 100 control volumes, with stretching used to concentrate control volumes in the near-wall region. The first computational node was placed at a location corresponding to $x_2^+ = 0.013$.

A previous study [8] considered mass transfer downstream of an abrupt pipe expansion. A low Reynolds number k-ε model and turbulent Schmidt number were used to predict the mass transfer coefficient at the wall. Numerical predictions were obtained for a constant turbulent Schmidt number of $\sigma_t = 0.9$, as well as for the case where $\sigma_t = 1.7$ for $x_2^+ < 5$. For this geometry, increasing the turbulent Schmidt number at the wall resulted in significantly better agreement with the experimental measurements. The present study also considered the effect of using a turbulent Schmidt number which increased near the wall, although in this case the relation of Kays and Crawford [6] was adopted.

The values predicted for the mass transfer coefficient, k_d, in fully developed channel flow are presented in Table 1. In this case, k_d was calculated from the predicted mass transfer flux at the wall and referenced to the difference between the bulk and wall concentrations. The discrepancy between the numerical results and the empirical correlation of Berger and Hau [7] is least for the case of a constant turbulent Schmidt number, in which case the difference is approximately 25 percent. This result contradicts that of the previous study [8]; however, for the abrupt expansion, the mass transfer coefficient was steadily decreasing in the streamwise direction, and fully developed conditions were not yet obtained.

Table 1
Mass transfer coefficient (m/s)

Experimental [7]	9.2×10^{-6}
Numerical:	
with constant $\sigma_t = 0.86$	7.1×10^{-6}
with variable σ_t [6]	5.7×10^{-6}

4. PLANE WALL JET

The second flow to be considered is a plane wall jet. The plane wall jet is a complex near-wall flow of both practical and theoretical significance. On the practical side, applications of wall jets include film-cooling in gas turbines and use of air streams to cool electronic equipment. On the theoretical side, a wall jet represents a basic flow pattern which combines attributes of both a free jet and a boundary layer. A plane wall jet essentially consists of a momentum driven jet directed parallel to a solid surface. The ambient flow can be either stagnant or consist of a weak co-flow. The wall jet is characterized by two shear regions, the inner layer due to the no-slip condition at the solid surface, and the outer layer due to the momentum exchange between the jet and ambient fluid. The review article of Launder and Rodi [9] summarizes the experimental data available.

With respect to near-wall turbulence models, a plane wall jet has two important features. Firstly, for a wall jet, the overlap region in which a logarithmic velocity profile might be expected to exist becomes very thin. This makes use of a wall function approach impractical. A second notable feature of the wall jet is the effect of the wall on the turbulence structure in the outer region. Experimental measurements indicate that the effect of the wall is to *damp* the turbulent motions normal to the wall, leading to a reduction in the shear stress in the outer region. This is thought to be related to the effect of the wall on the pressure fluctuation field. As such, the prediction of a plane wall jet is a test of the ability of a near-wall turbulence model to reproduce the reduction in turbulent transport due to both low Reynolds number and wall damping effects.

The present paper considers some aspects of a numerical prediction of a plane wall jet using various low Reynolds number k-ε models. The full two-dimensional form of the mean transport equations was retained, and the equation set solved elliptically following the finite volume method. The free boundary represented a stagnant ambient environment, while a no-slip condition was implemented along the wall. The upstream boundary was modelled as a wall, while a fully-developed outflow was used at the last downstream plane. The solution domain extended 120 slot-widths in the streamwise direction. The cartesian grid used approximately 5000 control volumes with the control volumes concentrated in the near-wall region. The first node was typically placed a distance of $x_2^+ = 3$ from the wall. Further details of the solution method are given in reference [10].

The Reynolds number of the wall jet based on the slot width was Re = 15,300. The primary set of experimental data used for comparison was that of Tailland [11]. The turbulence models considered included

the standard k-ε model with wall functions and the LRN k-ε models of Myong and Kasagi, both linear [3] and non-linear [4]. Due to space constraints, discussion will be limited to the numerical predictions for the skin friction, spread rate and Reynolds shear stress profile. The numerical predictions for the skin friction coefficient, $c_f = \tau_w / \frac{1}{2} \rho U_m^2$, based on the maximum velocity U_m, are compared to the values obtained from an empirical correlation for c_f [9] in Table 2. The use of a low Reynolds number formulation results in a substantial improvement over the wall function prediction, although the value is still somewhat higher than the experimental data.

Table 2
Skin friction coefficient for a wall jet at $x_1/b = 71$

Empirical correlation [9]	0.0072
Wall function	0.0110
Low Reynolds number model	
linear [3]	0.0083
non-linear [4]	0.0084

The numerical and experimental values of the spread rate, S, are presented in Table 3. The spread rate is defined to be $S = dy_h/dx_1$, where y_h is the half-width of the local mean velocity field. Based on the experimental data, the wall jet is known to have a spread rate which is approximately 30 percent lower than that of a free plane jet. The low Reynolds number models again offer significant improvement over a wall function approach. Nevertheless, the low Reynolds number predictions are still almost 10-15 percent too high.

Table 3
Spread rate for a plane wall jet

Free plane jet	0.110
Experimental [9]	0.073-0.076
Wall function	0.095
Low Reynolds number	
linear [3]	0.083
non-linear [4]	0.086

Finally, the numerical predictions for the Reynolds shear stress profile, $\langle u_1 u_2 \rangle$, are compared to the experimental data [11] in Figure 1. All of the numerical models substantially over predict the shear stress

profile in the outer region of the wall jet. (This is consistent with the fact that the numerical predictions for the spread rate were also too high.) From the figure, it is clear that the LRN k-ε models were not able to adequately reproduce the damping of the turbulent motions far from the wall.

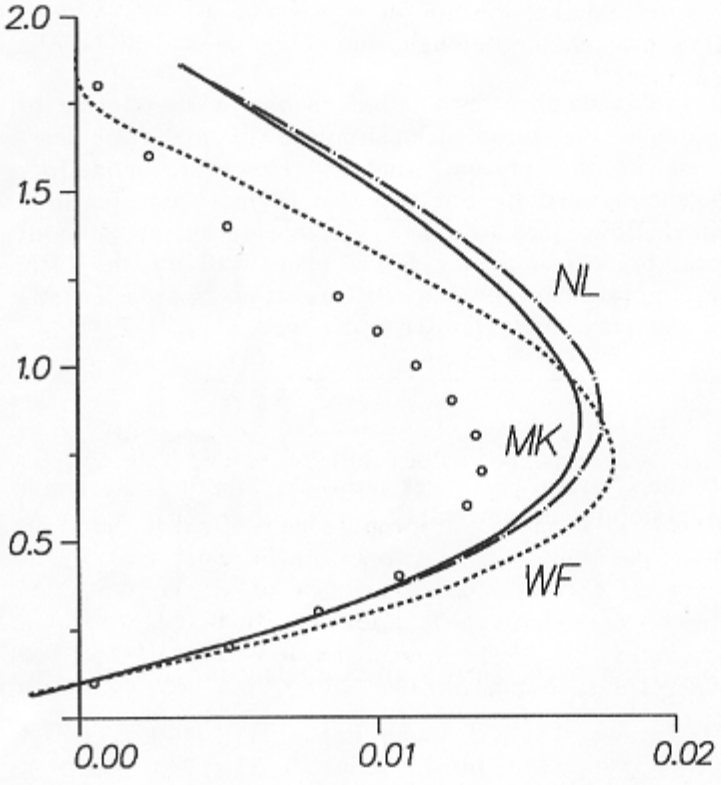

Figure 1. Reynolds shear stress profile in a plane wall jet.

The explanation for this deficiency is that the LRN models considered essentially model the total effect of the wall in terms of the low Reynolds number phenomenon. In actual fact, the reduction in the turbulent shear stress far from the wall is due to the damping of the large-scale inviscid motions perpendicular to the wall through the pressure field. From consideration of the production term in the transport equation for the Reynolds shear stress, i.e. $P_{12} = - \langle u_2 u_2 \rangle U_{1,2}$, it is clear that a reduction in the level of $\langle u_2 u_2 \rangle$ also results in a reduction in the production rate of $\langle u_1 u_2 \rangle$. The algebraic stress model

calculation of Ljuboja and Rodi [12] has previously demonstrated the capability of a Reynolds stress closure in this regard, albeit in a wall function context. The non-linear k-ε model, although capable of reproducing some degree of anisotropy in the normal stress components, did not capture the effect of wall damping via the pressure field.

5. CONCLUSIONS

Use of a low Reynolds number formulation enables a k-ε closure to more accurately reproduce the turbulence structure in the two near-wall flows considered in the present study. However, modelling questions and/or deficiencies remain. For the case of mass transfer in a fully developed channel flow, the use of a variable turbulent Schmidt number does not appear to be warranted. For a plane wall jet, the LRN formulation, while an improvement over a wall function approach, fails to reproduce the wall damping effect far from the wall.

6. ACKNOWLEDGEMENTS

The support of the Natural Sciences and Engineering Research Council of Canada is gratefully acknowledged.

7. REFERENCES

1 S.J. Kline and S.K. Robinson, Near-Wall Turbulence: Zoran Zaric Memorial Conf. (1988) 200.
2 Y. Nagano and M. Tagawa, ASME J. Fluids Engng., 112 (1990) 33.
3 H.K. Myong and N. Kasagi, JSME Int. J., Series III, 33 (1990) 63.
4 H.K. Myong and N. Kasagi, ASME J. Fluids Engng., 112 (1990) 521.
5 R.M.C. So, Y.G. Lai and H.S. Zhang, AIAA J., 29, No. 11 (1991) 1819.
6 W.M. Kays and M.E. Crawford, Convective Heat and Mass Transfer, McGraw-Hill, New York, 1980.
7 F.P. Berger and Y.-F. F.L. Hau, Int. J. Heat Mass Transfer, 20 (1977) 1185.
8 S. Nesic, J. Postlethwaite and D.J. Bergstrom, Int. J. Heat Mass Transfer, 35 (1992) 1977.
9 B.E. Launder and W. Rodi, Prog. Aeorosp. Sci., 19 (1981) 81.
10 J.W. Gu, M.Sc. Thesis, University of Saskatchewan (1992).
11 A. Tailland, Doctoral Thesis, Universite de Lyon (1970).
12 M. Ljuboja and W. Rodi, ASME J. Fluids Engng., 102 (1980) 350.